A single-photon sampling architecture for solid-state imaging sensors

Ewout van den Berg[*], Emmanuel Candès[†], Garry Chinn[‡], Craig Levin[§], Peter Olcott[¶], and Carlos Sing-Long[‖]

February 21, 2022

Abstract

Advances in solid-state technology have enabled the development of silicon photomultiplier sensor arrays capable of sensing individual photons. Combined with high-frequency time-to-digital converters (TDCs), this technology opens up the prospect of sensors capable of recording with high accuracy both the time and location of each detected photon. Such a capability could lead to significant improvements in imaging accuracy, especially for applications operating with low photon fluxes such as LiDAR and positron emission tomography.

The demands placed on on-chip readout circuitry imposes stringent trade-offs between fill factor and spatio-temporal resolution, causing many contemporary designs to severely under-utilize the technology's full potential. Concentrating on the low photon flux setting, this paper leverages results from group testing and proposes an architecture for a highly efficient readout of pixels using only a small number of TDCs, thereby also reducing both cost and power consumption. The design relies on a multiplexing technique based on binary interconnection matrices. We provide optimized instances of these matrices for various sensor parameters and give explicit upper and lower bounds on the number of TDCs required to uniquely decode a given maximum number of simultaneous photon arrivals.

To illustrate the strength of the proposed architecture, we note a typical digitization result of a 120 $\times$ 120 photodiode sensor on a 30 μm $\times$ 30 μm pitch with a 40 ps time resolution and an estimated fill factor of approximately 70%, using only 161 TDCs. The design guarantees registration and recovery of up to $s = 4$ simultaneous photon arrivals. A fast decoding algorithm is available, which decodes successfully with probability $1 - \alpha_s$ whenever $s > 4$. By contrast, a cross-strip design requires 240 TDCs and cannot uniquely decode any simultaneous photon arrivals. In a series of realistic simulations of scintillation events in clinical positron emission tomography the design was able to recover the spatio-temporal location of 98.6% of all photons that caused pixel firings.

1 Introduction

Photon detection has become an essential measurement technique in science and engineering. Indeed, applications such as positron emission tomography (PET), single-photon emission computed

[*]Department of Mathematics, Stanford University, Stanford CA 94305
[†]Departments of Mathematics and Statistics, Stanford University, Stanford CA 94305
[‡]Department of Radiology, Stanford University, Stanford CA 94305
[§]Departments of Radiology, Physics, Electrical Engineering, and Bioengineering, Stanford University, Stanford CA 94305
[¶]Departments of Radiology and Bioengineering, Stanford University, Stanford CA 94305
[‖]Institute for Computational and Mathematical Engineering, Stanford University, Stanford CA 94305

tomography, flow cytometry, LiDAR, fluorescence detection, confocal microscopy, and radiation detection all rely on accurate measurement of photon fluxes. Traditionally, the preferred measurement device has been the photomultiplier tube (PMT), which is a high-gain, low-noise photon detector with a high-frequency response and a large area of collection. In particular, it behaves as an ideal current generator for steady photon fluxes, making it suitable for use in applications in astronomy and medical imaging, among others. However, they are bulky, require manual assembly steps, and have limited spatial resolution for PET. For these reasons, extensive research has focused on finding feasible solid-state alternatives that can operate at much lower voltages, are immune to magnetic effects, have increased efficiency, and are smaller in physical size [43]. Recent designs have raised significant interest in the community, and their use as a replacement for PMTs in applications such as PET imaging [31], high-energy physics [48], astrophysics [52], LiDAR [3], and flow cytometry has been recently explored.

Silicon photomultiplier (SiPM) devices consist of two-dimensional arrays of Geiger avalanche photodiodes (APD) that are run above their breakdown voltage and are integrated with either an active or passive quenching circuit. Devices built up from these Geiger APD microcells are characterized by the fraction of sensing area on the device (the fill factor), and the fraction of incident photons that cause charged APDs to fire (the detection quantum efficiency). The product of these two quantities gives the combined photon detection efficiency (PDE).

The compatibility of Geiger APDs with standard CMOS technology has enabled a number of different designs. For example, the digital silicon photomultiplier (DSiPM) [27] adds processing circuitry to count the total number of photons hitting the sensor and records the time stamp of the first group of photons that crosses a predetermined photon intensity threshold. The resolution of the resulting sensor coincides with the size of the entire sensor (usually 3 mm $\times$ 3 mm in area) whereas the temporal sampling is limited to a single time stamp per pulse. Nevertheless, the sensor does achieve a very high fill factor (80%) and is, therefore, very sensitive. Note that in SiPM terminology, the above tiling of microcells into larger atomic units is often referred to as a pixel. Throughout this paper, however, we use the term pixel to refer to individual Geiger APD microcells, since they represent the smallest resolvable element in our proposed design.

An alternative sensor design, called SPAD, aims at a high temporal resolution and registers the time of each pixel (APD) firing [34, 40]. This is achieved by connecting each pixel to a high-performance time-to-digital converter (TDC), which records a time stamp in a memory buffer whenever a signal is detected on its input. Because of their relatively low complexity, especially when compared to analog-to-digital converters, TDCs allow the sensor to achieve an extremely high temporal resolution. However, the spatial resolution of the sensor is severely compromised by the large amount of support circuitry between neighboring pixels, resulting in an extremely low fill factor of approximately 1–5%.

Although promising, both designs show that current implementations highly underutilize the full potential of these silicon devices: due to the restricted chip area a trade-off must be made between the spatio-temporal resolution and the fill factor. In order to improve this trade-off, we take advantage of the special properties present in settings with a low photon flux. In particular, we claim that, by taking advantage of the temporal sparsity of the photon arrivals, we can increase the spatio-temporal resolution of the SiPM to within a fraction of the theoretical maximum while maintaining simple circuitry and a high fill factor.

This claim is made possible by the combination of two ideas: (1) to use TDCs as the main readout devices, and (2) to exploit ideas from *group testing* to reduce the number of these devices. As a motivational example, consider three possible designs for an $m \times m$ pixel grid. The first design, illustrated in Figure 1(a) corresponds to a design with a single TDC per pixel. This design can be

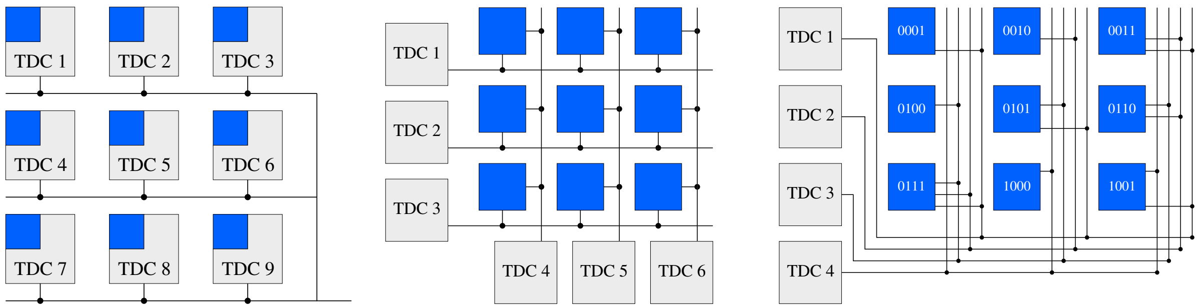

(a) (b) (c)

Figure 1: Three SiPM designs with (a) one TDC per pixel, (b) one TDC per row and column of pixels, and (c) one TDC per bit of the binary representation of each pixel number. The first design is capable of detecting any number of simultaneous hits, at the cost of a large number of TDCs. The other two can only uniquely decode up to a single pixel firing, but require substantially fewer TDCs.

seen as a trivial group test capable of detecting an arbitrary number of simultaneous firings, but at the cost of n^2 TDCs. When the photon flux is low, only a small number of pixels will typically fire at the same time[1], thus causing most TDCs to be idle most of the time, and resulting in a very poor usage of resources. The second design, shown in Figure 1(b), corresponds to the widely-used cross-strip architecture in which rows and columns of pixels are each aggregated into a single signal. This design requires only $2n$ TDCs, but information from the TDCs can only be uniquely decoded if no more than one pixel fired during the same time interval. Hinting at the power of more efficient group-testing designs, Figure 1(c) shows a design in which pixels are numbered from 1 to n^2 and in which a pixel i is connected to TDC j only if the j-th bit in the binary representation number i is one. This design is also capable of decoding up to a single pixel firing, but requires only $\lfloor \log_2 2n \rfloor$ TDCs. The objective of this paper is to show that whenever the number of simultaneous firings is small, a significant reduction in the number of TDCs (and accompanying memory buffers) can be attained by carefully selected designs, which reduce both the amount of overhead circuitry and the generated volume of data.

1.1 Contributions and paper organization

The main contribution of this paper are: (1) the introduction of group testing to the design of interconnection networks in imaging sensors, combined with TDC readout, (2) an architecture to time and locate photon arrivals, (3) the construction of highly optimized group testing matrices for a variety of conventional $m \times m$ grid sizes, (4) a comparison with alternative constructions, and (5) an extensive comparison with explicitly evaluated and optimized theoretical upper and lower bounds on the minimum number of TDCs required to decode an imaging sensor array.

The paper is organized as follows. We start by reviewing the concept of group testing and derive the currently best-known group testing designs for a range of grid sizes. We then provide an extensive survey of constructions used to obtain upper and lower bound on the minimum number of TDCs needed to guarantee recovery for $d = 2, \ldots, 6$ simultaneous hits. There, the results show that the designs generated earlier are close to the theoretical lower bounds. We then test the performance of the design on simulated data generated using a realistic model of scintillation events arising in

[1]Throughout the paper, firing at the same time is to be understood as within the same TDC sampling interval.

PET scanners. We conclude with a discussion on practical considerations in the implementation of the proposed design.

Throughout the paper we use the following notation: log is base e unless otherwise indicated; $[n]$ denotes the set $\{1, \ldots, n\}$; and $\binom{[n]}{k}$ denotes the family of all subsets of $[n]$ with k elements.

2 Group testing

Group testing was proposed by Dorfman [16] to effectively screen large numbers of blood samples for rare diseases (see [17] for more historical background). Instead of testing each sample individually, carefully chosen subsets of samples are pooled together and tested as a whole. If the test is negative, we immediately know that none of the samples in the pool is positive, saving a potentially large number of tests. Otherwise, one or more samples is positive and additional tests are needed to determine exactly which ones.

Since its introduction, group testing has been used in a variety of different applications including quality control and product testing [50], pattern matching [11, 33], DNA library screening [4, 18, 20, 41], multi-access communication [53], tracking of hot items in databases [13], and many others [17, 42]. Depending on the application, group testing can be applied in an adaptive fashion in which tests are designed based on the outcome of previous tests, and in a nonadaptive fashion in which the tests are fixed *a priori*. Additional variations include schemes that provide robustness against test errors [37, 38], or the presence of inhibitors [14, 26], which cause false positives and negatives, respectively.

In our SiPM application, each pixel fires independently[2] according to some Poisson process, and exactly fits in the probabilistic group-testing model [4]. Nevertheless, since we are interested in guaranteeing performance up to a certain level of simultaneous firings, we will study the application from a combinatorial group-testing perspective. Furthermore, measurements are necessarily nonadaptive as they are hardwired in the actual implementation. No error correction is needed; the only errors we can expect are spurious pixel firings (dark counts) or afterpulses, but these appear indistinguishable from real firings, and cannot be corrected for. The rate of these spurious pixel firings is usually much less than the signal rate, especially in our scintillation example [7].

2.1 Matrix representation and guarantees

A group test can be represented as a binary $t \times n$ incidence matrix or code A with t the length or number of tests and n the size or number of items, or pixels in our case. An entry $A_{i,j}$ is set to one if item j is pooled in test i, that is, if pixel j is connected to TDC i, and zero otherwise. Given a vector x of length n with $x_j = 1$ if item j is positive and zero otherwise, we can define the test vector y as $y = Ax$, where multiplication and addition are defined as logic AND and OR, respectively[3]. The columns a_j in A are called codewords, and for sake of convenience we allow set operations to be applied to these binary codewords, acting on or defining their support. As an illustration of the above, consider the following example:

[2] This assumes that pixels have been shielded to avoid cross-talk.

[3] Addition using the logic OR gives $0 + 0 = 0$ and $0 + 1 = 1 + 1 = 1$, while $0 \cdot 0 = 0 \cdot 1 = 0$ and $1 \cdot 1 = 1$, as usual.

$$
\begin{array}{ccccc}
 & & \begin{array}{ccccc} \mathit{1} & \mathit{2} & \mathit{3} & \mathit{4} & \mathit{5} \end{array} & & \\
\begin{pmatrix} 1 \\ 1 \\ 0 \end{pmatrix} & = & \begin{pmatrix} 1 & 0 & 0 & 1 & 1 \\ 0 & 1 & 0 & 1 & 0 \\ 1 & 0 & 1 & 0 & 0 \end{pmatrix} & & \begin{pmatrix} 0 \\ 1 \\ 0 \\ 1 \\ 0 \end{pmatrix} \\
y & = & A & & x
\end{array}
$$

In this example pixels 1, 4, and 5 are connected to the first TDC, as represented by the first row of A. When pixels 2 and 4 fire, we sum the corresponding columns and find that the first and second TDCs are activated, as indicated by y.

For group testing to be effective we want to have far fewer tests than items ($t \ll n$). This inherently means that not all vectors x can be reconstructed from y, so we will be interested in conditions that guarantee recovery when x has up to d positive entries.

The weakest notion for recovery is d-separability, which means that no combination of exactly d codewords can be expressed using any other combination of d codewords. A matrix is said to be $\bar{d}$-separable if the combination of any up to d codewords is unique. This immediately gives an information-theoretic lower bound on the length t:

$$t \geq \log_2 \left(\sum_{i=0}^{d} \binom{n}{i} \right). \tag{1}$$

When d is small compared to n, this gives $t \approx d \log_2(n/d)$. A stronger criteria is given by d-disjunctness. Given any two codewords u and v, we say that u covers v if $u \cup v = u$. Based on this, define A to be d-disjunct if no codeword in A is covered by the union of any d others. The concept of disjunctness of sets and codes has been proposed in a number of settings and such codes are also known as superimposed codes [36], or d-cover free families [24]. The advantage of d-disjunct codes is that the positive entries in any d-sparse vector x correspond exactly to those codewords in A that remain after discarding all codewords that have a one in a position where y is zero. This is unlike general separable matrices, where a combinatorial search may be needed for the decoding.

The central goal in group testing is to determine the smallest length t for which a matrix of size n can satisfy certain separability or disjunctness properties. Denote by $S(n, d)$ and $D(n, d)$ the set of all $t \times n$ matrices A that are d-separable, respectively d-disjunct. Then we can define $T_S(n, d)$ the smallest length of any $A \in S(n, d)$, and likewise for $T_D(n, d)$. As a further refinement in classification we define $D_w(n, d)$ as all constant-weight d-disjunct matrices of size n, i.e., those matrices whose columns all have the same weight or number of nonzero entries (note that the weights of any two matrices within this class can differ). The overlap between any two columns a_i and a_j of a code is defined as $|a_i \cap a_j|$. Consider a constant-weight w code A with maximum pairwise overlap

$$\mu = \mu(A) := \max_{i \neq j} |a_i \cap a_j|.$$

It is easily seen that it takes $\lceil w/\mu \rceil$ columns to cover another one, and therefore that

$$d \geq \left\lfloor \frac{w-1}{\mu} \right\rfloor. \tag{2}$$

We can then define $D_{w,\mu}(n, d)$ as the class of constant-weight codes of size n where the right-hand side of (2) equals d. As for all other classes, the actual disjunctness of the codes in $D_{w,\mu}$ may still be higher, however, there is a subtle distinction in parameterization here in that, by definition, we have $D_{w,\mu}(n,d+1) \cap D_{w,\mu}(n,d) = \emptyset$, whereas $D_w(n,d+1) \subset D_w(n,d)$, and likewise for D and S. Summarizing, we have

$$D_{w,\mu}(n,d) \subseteq D_w(n,d) \subseteq D(n,d) \subseteq S(n,d),$$

along with the associated minimum lengths $T(n,d)$.

2.2 Matrix construction

In this section we discuss three methods for creating d-disjunct binary matrices. In addition, we construct matrices for the particular case where $n = 3{,}600$, corresponding to a 60×60 pixel array.

2.2.1 Greedy approach

The greedy approach generates d-disjunct matrices one column at a time. For the construction of a constant-weight w matrix of length t the algorithms starts with $\mathcal{F} = \emptyset$, and proceeds by repeatedly drawing, uniformly at random, an element F from $\binom{[t]}{w}$ as a candidate column. Whenever the distance to all sets already in $\mathcal{F}$ exceeds w/d we add F to $\mathcal{F}$ and continue the algorithm with the updated family. This process continues until either $|\mathcal{F}| = n$ or a given amount of time has passed.

We applied the greedy algorithm to construct d-disjunct matrices of size at least 3,600. For each value of d and length t, the algorithm was allowed to run for 12 hours. Row (l) of Table 3 gives the minimum t for which the algorithm found a solution. Instances with fewer rows are very well possible; this strongly depend both on the choice of the initial few columns and the amount of time available.

A further reduction in the code length could be achieved by checking disjunctness in a groupwise, rather than a pairwise setting. However, the number of possible d-subsets of columns to consider at each iteration grows exponentially in d, thereby rendering this approach intractable for even moderate values of d.

2.2.2 Chinese remainder sieve

Eppstein et al. [22] recently proposed the 'Chinese remainder sieve', a number-theoretic method for the deterministic construction of d-disjunct matrices. In order to generate a d-disjunct matrix with at least n columns, first choose a sequence $\{p_1^{e_1}, p_2^{e_2}, \ldots, p_k^{e_k}\}$ of powers of distinct primes such that $\prod_{i=1}^{k} p_i^{e_i} \geq n^d$. A $t \times n$ matrix A with $t = \sum_{i=1}^{k} p_i^{e_i}$ is then created by vertical concatenation of $p_\ell^{e_\ell} \times n$ matrices A_ℓ as follows:

$$A = \begin{bmatrix} A_1 \\ A_2 \\ \vdots \\ A_k \end{bmatrix}, \qquad A_\ell(i,j) = \begin{cases} 1 & i \equiv j \mod p_\ell^{e_\ell} \\ 0 & \text{otherwise.} \end{cases}$$

As an example, consider the construction of a 1-disjunct 5×6 matrix generated based on $p_1 = 2$ and $p_2 = 3$. Applying the above definition we obtain:

$$A = \left[\begin{array}{c} A_1 \\ \hline A_2 \end{array}\right] = \left[\begin{array}{cccccc} 1 & 0 & 1 & 0 & 1 & 0 \\ 0 & 1 & 0 & 1 & 0 & 1 \\ \hline 1 & 0 & 0 & 1 & 0 & 0 \\ 0 & 1 & 0 & 0 & 1 & 0 \\ 0 & 0 & 1 & 0 & 0 & 1 \end{array}\right].$$

d	t	n	prime powers
2	82	4077	$\{2^3, 3^2, 5, 7, 11, 13, 17, 23\}$
3	155	3855	$\{2^2, 3, 5, 7, 11, 13, 17, 19, 23, 29, 37\}$
4	237	3631	$\{2^3, 3, 5, 7, 11, 13, 17, 19, 23, 29, 31, 37, 43\}$
5	333	4023	$\{2^3, 3^2, 5, 7, 11, 13, 17, 19, 23, 29, 31, 37, 41, 43, 53\}$
6	445	4077	$\{2^3, 3^2, 5, 7, 11, 13, 17, 19, 23, 29, 31, 37, 41, 43, 53, 61\}$

Table 1: Prime powers used for the construction of d-disjunct $t \times n$.

The above construction requires $t = \mathcal{O}(d^2 \log^2 n/(\log d + \log\log n))$ rows for a d-disjunct matrix of size n [22]. This is only slightly worse than the best-known $\mathcal{O}(d^2 \log n)$ construction, which we discuss in more detail in Section 3.1. Using a near-exhaustive search over prime-power combinations, we construct d-disjunct matrices of size at least 3,600. The parameters giving designs with the smallest number of rows are given in Table 1.

2.2.3 Designs based on error-correcting codes

Excellent practical superimposed codes can be constructed based on error-correcting codes. Here, we discuss a number of techniques and constructions we used to generate the best superimposed codes known to us for a variety of pixel array sizes (i.e, for square $m \times m$ arrays with $m \in \{10, 20, 30, 40, 60, 120\}$). For comparison with other constructions, the results are summarized in Table 2, and in row (n) of Table 3 for $n = 3{,}600$.

Binary codes. The most straightforward way of obtaining d-disjunct superimposed codes is by simply taking constant-weight binary error-correction codes obeying (2), with overlap μ as given below. The on-line repository [6] lists the best known lower bound on maximum size $A(n, d, w)$ for constant weight w codes of length n and Hamming distance d (note the different use of n and d in this context). Given a code $\textsc{st}$(n,d,w) from this Standard Table, the overlap satisfies $\mu \leq w - d/2$. Some codes are given explicitly, whereas others require some more work to instantiate. We discuss two of the most common constructions that are used to instantiate all but one of the remaining codes we use. The first construction consists of a short list of seed codewords v_i, along with a number of cyclic permutations. These permutations give rise to a permutation group $\mathcal{P}$ and the words in the final code are those in the union of orbits of the seed vectors: $\cup_i \{w \mid w = P(v_i), P \in \mathcal{P}\}$. The second construction shortens existing codes in one of two ways. We illustrate them based on the generation of the 2-disjunct code $\textsc{st}$(21,8,7) of size 100 from $\textsc{st}$(24,8,8). The first type of shortening consists of identifying a row i with the most ones and then selecting all columns incident to this row and deleting row i. This both reduces the weight and the length of the code by one, but preserves the distance, and in this case gives $\textsc{st}$(23,8,7) (note that shortenings do not in general lead to new optimal or best known codes). The second type of shortening identifies a row i with the most zero entries and creates a new code by keeping only the columns with a zero in the i-th row, and then removing the row. This construction does not affect the weight of the matrix, only the size and length. Repeating this twice from $\textsc{st}$(23,8,7) yields the desired $\textsc{st}$(21,8,7) code. Note that for constant-weight codes, the minimum number of ones in any given row is bounded above by $\lfloor wn/t \rfloor$. This expression can be used to give a theoretical minimum on the number of rows by which we can shorten a code. In practice it may be possible to remove a substantially larger number of rows. Below we will frequently use shortening to obtain codes with smaller length. In these cases we only use the second type of shortening, based on zero entries.

q-ary error-correction codes. The Standard Table only lists codes with relatively small lengths and consequently, limited sizes. In order to construct larger or heavier codes we apply a construction based on (maximal distance separable (MDS)) q-ary error-correcting codes, as proposed by Kautz and Singleton [36]. Let $(n, k, d)_q$ denote a linear q-ary code of length n, size q^k, and Hamming distance d. Each codeword in these codes consists of n elements taken from GF(q) and differs in at least d locations from all other codewords. A binary superimposed code can be obtained from these q-ary codes by replacing each element with a corresponding column of a $q \times q$ identity matrix I_q. That is, we map each element in GF(q) to a unique column of I_q. For example, we map value k to the $(k+1)$-st column of I_q as follows:

q-ary		2	0	1	2	1	1	0
	0	0	1	0	0	0	0	1
binary	1	0	0	1	0	1	1	0
	2	1	0	0	1	0	0	0

The overlap between any two codewords of the resulting concatenated code is bounded by the length of the code n minus the distance d. Meanwhile, the weight is exactly the length. The disjunctness of the resulting code is therefore at least $\lceil (n-1)/(n-d) \rceil$. As an aside, note that this construction requires an explicit set of codewords. This can be contrasted with q-ary error-correction codes, for which fast encoding-decoding algorithms often exist, and which do not require such an explicit representation.

Existence of a large class of $(n, k, d)_q$ codes, including the well-known Reed-Solomon codes is shown by Singleton [36, 49]. In MacWilliams and Sloane [39, Ch. 11, Thm. 9] cyclic MDS codes with $n = q+1$ and $d = q-k+2$ are shown to exist whenever $1 \leq k \leq q+1$ and q is a prime power. As a result, it can be concluded that, when expressed in group-testing notation, this concatenated code construction requires a length $t = \mathcal{O}(\min[n, k^2 \log^2 n])$ [42], compared to the best-known bound of $\mathcal{O}(k^2 \log n)$. Despite the slightly weaker bound, we shall see below that for small instances, the resulting codes are far superior to the random constructions used to yield the improved bound.

As an example, we used a concatenation of $(10, 4, 7)_{11}$ with I_{11}, denoted $(10, 4, 7)_{11}^{I_q}$, to construct the 3-disjunct matrix of size $n = 14{,}400$ shown in Table 2. Most of the other codes obtained using this construction have an additional superscript $s(k)$ to indicate the application of k shortening steps. The 4-disjunct code of length $n = 1{,}600$ also has a superscript x to indicate extension of the code. In this case, the four shortening steps resulted in a $113 \times 1{,}596$ code, falling just short of the desired size of 1,600. The very structured nature of these concatenated codes means that many constant-weight vectors are not included, even if they may be feasible. We can therefore try to apply greedy search techniques to augment the code. For this particular case it was found to be relatively easy to add several columns, thus resulting in a code of desired size.

All of the q-ary codes appearing in Table 2 are Reed-Solomon codes, except for $(10, 4, 7)_9$, which is a constacyclic linear code whose construction is given by [30].

General concatenated codes. As mentioned by Kautz and Singleton [36], it is possible to replace the trivial identity code by arbitrary d-disjunct binary matrices in forming concatenated codes, provided that the size of the matrix is at least q. This construction is extensively used by D'yachkov *et al.* [19] to form previously unknown instances of superimposed codes. We also investigated this approach and found that the concatenation of the $(7, 4, 4)_{11}$ code with ST(9,4,3) yielded our smallest 2-disjunct code of size 14,400. Likewise a 2-disjunct $51 \times 4{,}489$ matrix can be obtained by concatenating $(3, 2, 2)_{67}$ with ST(17,6,5). The code given in Table 2 lists instead

	$n = 100$		$n = 400$		$n = 900$	
d	t	construction	t	construction	t	construction
2	21	ST(21,8,7)	31	ST(31,8,7)	38	ST(38,8,7)
3	36	ST(36,10,7)	51	ST(51,10,7)	73	$(7,3,5)_{11}^{I_q,s(4)}$
4	48	ST(48,8,5)	64	C$(65,9,3)^{s(1)}$	95	$(9,3,7)_{11}^{I_q,s(4)}$
5	60	ST(60,10,6)	107	$(11,3,9)_{11}^{I_q,s(14)}$	117	$(11,3,9)_{11}^{I_q,s(4)}$
6	75	$(7,2,6)_{11}^{I_q,s(2)}$	144	$(13,3,11)_{13}^{I_q,s(25)}$	156	$(13,3,11)_{13}^{I_q,s(13)}$

	$n = 1{,}600$		$n = 3{,}600$		$n = 14{,}400$	
d	t	construction	t	construction	t	construction
2	44	ST(44,8,7)	51	ST(51,8,7)	63	$(7,4,4)_{11}^{\mathrm{ST}(9,4,3)}$
3	78	$(10,4,7)_{9}^{I_q,s(12)}$	85	$(10,4,7)_{9}^{I_q,s(5)}$	110	$(10,4,7)_{11}^{I_q}$
4	113	$(9,3,7)_{13}^{I_q,s(4),x}$	142	$(9,3,7)_{16}^{I_q,s(2)}$	161	$(13,4,10)_{13}^{I_q,s(8)}$
5	140	$(11,3,9)_{13}^{I_q,s(3)}$	174	$(11,3,9)_{16}^{I_q,s(2)}$	233	$(16,4,13)_{16}^{I_q,s(23)}$
6	166	$(13,3,11)_{13}^{I_q,s(3)}$	206	$(13,3,11)_{16}^{I_q,s(2)}$	323	$(13,3,11)_{25}^{I_q,s(2)}$

Table 2: Overview of best-known constructions for d-disjunct matrices of size n. Codes from the Standard Table [6] and covering are indicated by ST$(\cdot)$ and C$(\cdot)$; all other entries are $(n,k,d)_q$ codes. Superscripts $s(k)$ indicates a shortening of k steps with pivoting on zero entries; x indicates a greedy extension, I_q indicates concatenation with a $q \times q$ identity matrix. The ST$(\cdot)$ superscript indicates concatenation with a binary code from the Standard Table.

ST(51,8,7), which yields a slightly smaller code with weight 7 instead of 15. Note that concatenation with non-trivial disjunct matrices can result in codes in $D_w(d,n) \setminus D_{w,\mu}(d,n)$ or even $D(d,n) \setminus D_w(d,n)$.

Other constructions. We would like to mention two other construction techniques that can be used to generate superimposed codes. The first technique is based on certain designs such as t-designs and Steiner systems [12], which were used for example by Balding *et al.* [4] to construct a 4-disjunct 65×520 binary code. The matrix corresponding to this particular system can be found on-line in the La Jolla Covering Repository [29] as $C(65,9,3)$. In Table 2 we shorten this matrix by a single row to obtain a code for $n = 400$. Although this construction is significantly shorter than the best q-ary based design we could find (a 76×408 shortening of $(9,3,7)_9$), it is typically much harder to obtain explicit instantiations of designs, or even to show their existence, at least compared to q-ary codes. The second technique based on Latin squares appears in [36], and was used by D'yachkov *et al.* [19] to create 2-disjunct $51 \times 4{,}624$ and $63 \times 14{,}400$ matrices.

3 Theoretical bounds

We now summarize an extensive literature concerning theoretical bounds on the minimum number of pools required for a group-testing design of size n to be d-disjunct. These results include both upper and lower bounds on this minimum, and can be used to get an idea about the quality of the matrices we constructed in the previous section.

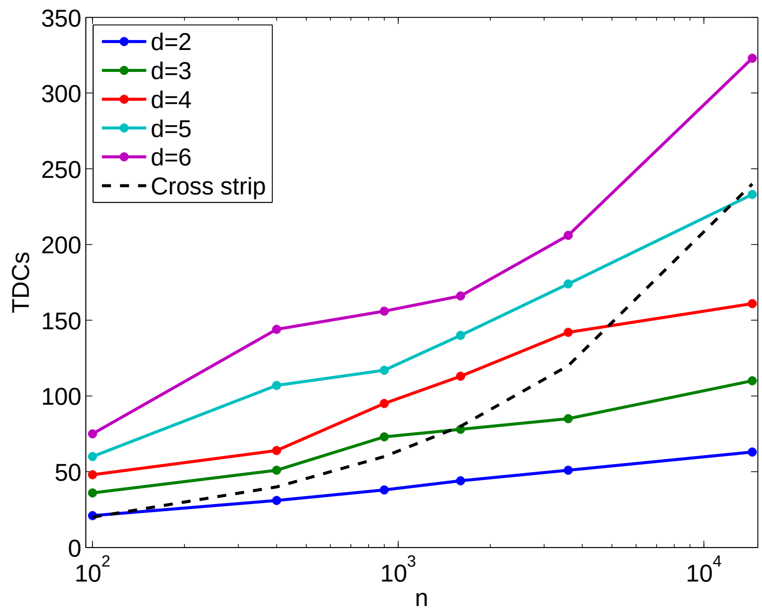

Figure 2: Comparison between the number of TDCs used for the best-known codes in Table 2 and a standard cross-strip design, for different numbers of pixels n. The cross-strip design connects each row and column to a single TDC, giving a $d = 1$ disjunct encoding. The number of TDCs in the cross-strip design grows as $\mathcal{O}(\sqrt{n})$, much faster than the $\mathcal{O}(d^2 \log n)$ in group-testing matrices.

3.1 Asymptotic bounds

Bounds on the growth rate of $T_D(n, d)$ have been discovered and rediscovered in different contexts in information theory, combinatorics, and group testing [47]. In the context of superimposed codes, D'yachkov and Rykov [21] obtained the following bounds:

$$\Omega(d^2 \log n/ \log d) \leq T_D(n, d) \leq \mathcal{O}(d^2 \log n).$$

Ruszinkó [47] and Füredi [28] give an interesting account on the lower bound and provide simpler proofs. The lower bound was also obtained for sufficiently large d with $d \leq n^{1/3}$ by Chaudhuri and Radhakrishnan [8] in the context of d-cover free systems for system complexity, which was extended to the general case by Clementi *et al.* [10].

For the upper bound, it follows from the analysis of a greedy-type construction given by Hwang and Sós [32], that for $t \geq 16d^2$ we have

$$T_{D_{w,\mu}}(n, d) \leq 16d^2 \cdot \log_3(2) \cdot (\log_2(n) - 1) < 11d^2 \log_2(n). \tag{3}$$

An efficient polynomial-time algorithm for generating similar constant-weight d-disjunct $t \times n$ matrices with $t = \mathcal{O}(d^2 \log n)$ was given by Porat and Rothschild [42].

3.2 Non-asymptotic results

When working with particular values of d and n, constants in theoretic bounds become crucial. Most theoretical results, however, are concerned with growth rates and even if explicit constants are given, such as those in (3), they may be too loose to be of practical use.

In this section we are interested in the code length t required to guarantee the unique recovery of up to $d = 6$ simultaneous firings on a 60×60 pixel array, that is n =3,600. We do this by studying the various models used to obtain upper and lower bounds on $T(n,d)$ and numerically evaluating the original expressions, instead of bounding them. By optimizing over parameters such as weight or matrix size, we obtain the best numerical values for the bounds, as permitted by the different models. These will be used as a reference point to evaluate the quality of the codes given in Table 2.

All bounds are evaluated using Sage [51] and summarized in Table 3 for $d = 2, \dots, 6$. We omit results for $d = 1$, which only requires the columns of the matrix to be unique.

3.2.1 Upper bounds on $T(n,d)$

The construction of a d-disjunct binary $t \times n$ matrix, or providing an algorithm for doing so, immediately yields t as an upper bound for one of the $T(n,d)$ values. In the literature there are three main techniques to obtain d-disjunct matrices of various sizes; we discuss each of these in the following paragraphs.

Sequential picking. The construction given by Hwang and Sós [32] for obtaining an upper bound on $T_{D_{w,\mu}}(n,d)$ works as follows. Starting with a family of initially all good sets $G_0 = \binom{[t]}{w}$ of a fixed weight w we pick a random element $g \in G_0$. After we make this choice we determine the family B_1 of sets in G_0 whose overlap with g is w/d or more (this includes g itself). We then remove all the bad items B_1 from G_0 to get $G_1 = G_0 \setminus B_1$. We then repeat the procedure, picking at each point a g from G_i, determining B_{i+1} and forming G_{i+1}, until G_n is empty. We can then form a $t \times n$ matrix A with the support of each column corresponding to one of the selected g. This matrix will be d-disjunct since, by construction, it has constant column weight w and satisfies (2) with overlap $\mu < w/d$. For the number of rows in A, notice that the size of each B_i satisfies

$$|B_i| \leq \sum_{i=\lceil w/d \rceil}^{w} \binom{w}{i}\binom{t-w}{w-i}$$

Because the size of the initial family G_0 was $\binom{t}{w}$ we have that

$$n \geq \binom{t}{w} \Bigg/ \sum_{i=\lceil w/d \rceil}^{w} \binom{w}{i}\binom{t-w}{w-i}. \tag{4}$$

This can be turned into the upper bound on $T_{D_{w,\mu}}(n,d)$ shown in (3) by following the parameter choice and analysis given in [32]. Essentially the same argument was used earlier by Erdös *et al.* to prove an alternative bound given in [24, Proposition 2.1]. Entries (a–c) in Table 3 are obtained using respectively (3), the bound given in [24] with optimal choice of w, and the smallest t that satisfies (4) for some $w \leq t$ (see also [15, p. 232]).

Random ensemble. An alternative to picking compatible columns one at a time, is to draw an entire set of columns from a suitable distribution and check if the resulting matrix is indeed d-disjunct. An upper bound on the required number of rows is obtained by finding the smallest t such that the probability that the matrix does not satisfy d-disjunctness is strictly bounded above by one.

Consider a $t \times n$ matrix A with entries drawn i.i.d. from the Bernoulli distribution; each entry takes on the value 1 with probability β and the value 0 with probability $1-\beta$. For any column in A, the probability that it is covered by $d < n$ of the other columns is given by

$$p = (1 - \beta(1-\beta)^d)^t, \tag{5}$$

since each entry in the column is not covered by the union of the other d if and only if its value is 1, and the corresponding entries in the other d columns are all 0. Since we want to minimize the chance of overlap, we find the minimum with respect to β, giving $\beta = 1/(d+1)$. By taking a union bound over all possible sets, we can bound the probability that at least one column in A is covered by some d others as

$$P(A \text{ not } d\text{--disjunct}) \leq n\binom{n-1}{d}p. \tag{6}$$

This setup forms the basis for the analysis given by D'yachkov and Rykov [21]. In Table 3, row (d), we show the smallest t for which this probability is less than one; for the optimal β, this is given by

$$t = \left\lfloor 1 - \log\left(n\binom{n-1}{d}\right) \Big/ \log\left(1 - \frac{d^d}{(d+1)^{d+1}}\right)\right\rfloor.$$

To construct matrices with constant-weight w, we can uniformly draw columns from $S = \binom{[t]}{w}$. The probability that a fixed column is covered by d others can be evaluated as follows. Let $R_d(t, w, i)$ denote the number of ways we can cover a fixed set of w entries in a t-length vector with d columns, given that i entries have already been covered. With only a single column left, we first cover the remaining $w - i$ entries, leaving i entries to be freely selected in the remaining $t - (w - i)$ positions. This gives

$$R_1(t, w, i) = \binom{t-w+i}{i}.$$

For $d > 1$ we can cover up to $w - i$ entries and cover the others using the remaining $d - 1$ columns. Therefore,

$$R_d(t, w, i) = \sum_{j=0}^{w-i}\binom{w-i}{j}\binom{t-w+j}{w-j}R_{d-1}(t, w, i+j).$$

The probability that a column is covered by d others is then given by

$$p = R_d(t, w, 0) \Big/ \binom{t}{w}^d, \tag{7}$$

and we can again use the union bound given by (6). In order to determine the smallest possible t we start at $t = 1$ and double its value until the right-hand side of (6) is less than one and then use binary search to find the desired t. This is repeated for all suitable column weights w and row (e) of Table 3 lists the smallest value of t obtained using this procedure.

The use of the union bound in (6) ignores the fact that many of the columns and d-sets are independent. In order to obtain sharper bounds for a similar problem, we follow Yeh [54] and apply Lovász Local Lemma [25], stated in [2, Corollary 5.1.2].

Lemma 3.1 (The Local Lemma; Symmetric case) *Let E_1, E_2,…,E_n be events in an arbitrary probability space. Suppose that each event E_i is independent of all other events E_j except at most μ of them, and that $P(E_i) \leq p$ for all $1 \leq i \leq n$. If*

$$ep(\mu + 1) \leq 1 \tag{8}$$

then $P(\cap_{i=1}^{n} \bar{E}_i) > 0$.

Working again with n columns drawn uniformly and independently from $\binom{[t]}{n}$, let $E_{i,J}$ denote the event that column i is covered by the set J of d other columns. Any event E_{i_1,J_1} is independent from E_{i_2,J_2} whenever $(J_1 \cup \{i_1\}) \cap (J_2 \cup \{i_2\}) = \emptyset$, and the number of events μ that violate this condition is given by

$$\mu = (d+1)\left[\binom{n}{d+1} - \binom{n-d-1}{d+1}\right].$$

All we then need to do is find the smallest t for which, with an optimal choice of w, condition (8) is satisfied using p as given in (7). That is, find a t such that

$$e \cdot R_d(t,w,0)\binom{t}{w}^{-d}(\mu+1) \leq 1.$$

The results obtained by this method are given in row (f) in Table 3. We omit similar results obtained using a Bernoulli model, or the q-ary construction considered by Yeh [54], since they give larger values of t.

Random selection with post processing. A third approach to generating d-disjunct matrices is to start with a $t \times m$ matrix with $m \geq n$, drawn from a certain random ensemble, and randomly mark for deletion one of each pair of columns whose overlap is too large. Whenever the expected number of columns marked for deletion is strictly less than $n-m+1$ we can be sure that a d-disjunct $t \times n$ matrix exists and can be generated using this approach. (Note that some of the approaches described in the previous paragraph are a special case of this with $m = n$.) A variation on this approach is to pick a column and mark it for deletion if there exist any other d columns that cover it. Starting with this latter approach for the Bernoulli model with $\beta = 1/(d+1)$, a bound on the probability of a column being marked is found by applying a union bound to (5):

$$P(\text{covered}) \leq \binom{m-1}{d}\left(1 - \frac{d^d}{(d+1)^{d+1}}\right)^t.$$

The expected number of columns marked is then bounded by

$$\mathbb{E}(\#\text{cols}) = m \cdot P(\text{covered}) \leq m\binom{m-1}{d}\left(1 - \frac{d^d}{(d+1)^{d+1}}\right)^t,$$

and the smallest t for which the left-hand side of this inequality is strictly less than $m-n+1$ is given in row (g) of Table 3. A similar derivation based on constraints on the pairwise overlap of columns can easily be seen to yield

$$\mathbb{E}(\#\text{columns marked}) \leq \binom{m}{2} \cdot \binom{t}{w}^{-1} \sum_{i=\lceil w/d \rceil}^{w} \binom{w}{i}\binom{t-w}{w-i},$$

which leads to the results shown in row (h). The best results for $T_D(n,d)$ based on bounds of the probabilistic method in row (i) were obtained for groupwise covering of constant weight vectors, a model which was studied earlier by Riccio and Colbourn [45]. For completeness we list in row (j) the results based on a random q-ary construction similar to the one we discussed earlier. A final method we would like to mention chooses $m = n$, but instead of removing marked columns, it augments the matrix with the identity matrix below all marked columns, thus fixing a (potential) violation of d-disjunctness by increasing the number of rows. The results of this method by Yeh [54] are presented in row (k).

	Bound $\setminus$ d	2	3	4	5	6	Reference and comments
	Upper bounds (theoretical)						
(a)	$T_{D_{w,\mu}}(n,d) \leq$	436	982	1746	2729	3929	Adaptation of [32] given in (3)
(b)	$T_{D_{w,\mu}}(n,d) \leq$	94	237	443	711	1043	[24, Proposition 2.1] with optimal w
(c)	$T_{D_{w,\mu}}(n,d) \leq$	**90**	**222**	**412**	**660**	**966**	Equation (4) with optimal w
(d)	$T_D(n,d) \leq$	149	278	442	640	870	Bernoulli, [21, Theorem 5]
(e)	$T_{D_w}(n,d) \leq$	96	190	312	459	631	Constant weight, groupwise cover
(f)	$T_{D_w}(n,d) \leq$	76	163	279	422	590	Constant weight, Lovász local lemma
(g)	$T_D(n,w) \leq$	110	225	376	561	779	Bernoulli, groupwise cover
(h)	$T_{D_{w,\mu}}(n,d) \leq$	99	249	465	746	1094	Constant weight, pairwise overlap
(i)	$T_{D_w}(n,d) \leq$	**71**	**154**	**265**	**402**	**565**	Constant weight, groupwise cover; see [45]
(j)	$T_{D_{w,\mu}}(n,d) \leq$	130	300	522	828	1178	Adaptation of [9, Algorithm 1]
(k)	$T_D(n,d) \leq$	98	205	348	524	734	[54, Theorem 2.6]
	Upper bounds (instances)						
(l)	$T_{D_{w,\mu}}(n,d) \leq$	58	132	224	345	484	Greedy search
(m)	$T_{D_w}(n,d) \leq$	82	155	237	333	445	[22, Section 2]; see Table 1
(n)	$T_{D_{w,\mu}}(n,d) \leq$	51	85	142	174	206	Error-correction code based
	Lower bounds						
(o)	$T_{D_{w,\mu}}(n,d) \geq$	**35**	**56**	**75**	**96**	**115**	[35, Theorem 2]
(p)	$T_{D_{w,\mu}}(n,d) \geq$	35	55	74	93	113	[36, Equation 5] and [21, Equation 18]
(q)	$T_{D_w}(n,d) \geq$	**35**	–	–	–	–	[23, Theorem 1]
(r)	$T_{D_{w,\mu}}(n,d) \geq$	32	48	62	75	88	[24, Proposition 2.1]
(s)	$T_{D_w}(n,d) \geq$	29	**40**	**48**	**55**	61	[47, Lemma 3.2]
(t)	$T_S(n,d) \geq$	**23**	**33**	**43**	**53**	**62**	Information theoretical lower bound

Table 3: Upper and lower bounds on the minimum number of rows needed for a d-disjunct or $\bar{d}$-separable matrix with $n = 3600$ rows. Entries shown in boldface denote the best theoretical upper and lower bounds we could find for each of the given classes.

Remarks on the upper bounds. Even though different models may lead to the same growth rates in $T(n,d)$, there is a substantial difference in resulting values, when numerically evaluated. The groupwise models easily outperform bounds based on pairwise comparison overlap. In addition there is a large gap between matrices with constant-weight columns, and those generated with i.i.d. Bernoulli entries, the former giving much more favorable results. The second approach given above, based on drawing fixed $t \times n$ matrices is clearly outperformed by the third approach in which a $t \times m$ matrix is screened and reduced in size by removing columns that violate disjunctness or maximum overlap conditions, even if the Lovász Local Lemma is used to sharpen the bounds.

3.3 Lower bounds on $\mathbf{T(n,d)}$

Most of the lower bounds listed in Table 3 are derived using the concept of a *private set*. Let $\mathcal{F}$ be a family of sets (the columns of our matrix A). Then T is a private set of $F \in \mathcal{F}$, if $T \subseteq F$, and T is not included in any of the other sets in $\mathcal{F}$. For $\mathcal{F} \in D_{w,\mu}(n,d)$ with length t, constant column weight w, and maximum overlap μ, it is easily seen that, by definition, each $(\mu+1)$-subset of $F \in \mathcal{F}$ is private. The number of such private sets $|\mathcal{F}| \cdot \binom{w}{\mu+1}$ cannot exceed the total number of these sets, $\binom{t}{\mu+1}$, and it therefore follows [21, 36] that

$$|\mathcal{F}| \leq \binom{t}{\mu+1} \Big/ \binom{w}{\mu+1}.$$

Based on this we can find the smallest t for which there are values w and μ obeying $(w-1)/\mu \geq d$, such that the right-hand side of the above inequality exceeds the desired matrix size. This gives a lower bound on the required code length and the resulting values are listed in row (p) of Table 3. A slightly better bound on the same class of matrices follows from an elegant argument due to Johnson [35], and is given in row (o).

Ruszinkó [47] studies d-disjunctness in constant-weight matrices without considering maximum overlap and provides the following argument. Let $\mathcal{F} \in D_w(n,d)$ be a family of w-subsets in $[t]$, such that no d sets in $\mathcal{F}$ cover any other set. Moreover, assume that $w = kd$ for some integer k. Any $F \in \mathcal{F}$ can be partitioned into d sets of length k, and it follows from the d-disjunctness of $\mathcal{F}$ that at least one of these d subsets is private to F (otherwise it would be possible to cover F with d other columns). The key observation then, is that Baranyai's Theorem [5] guarantees the existence of $s = \binom{w}{w/d}/d$ different partitions of F such that no subset in the partitions is repeated. Each of these s partitions contains a private set, so the total number of private sets is at least $|\mathcal{F}| \cdot s$. Rewriting this gives

$$|\mathcal{F}| \leq d\binom{t}{w/d} \Big/ \binom{w}{w/d}.$$

With proper rounding this can be extended to general weights w, giving the results shown in row (s). The results in rows (q) and (r) are also obtained based on private sets, but we will omit the exact arguments used here. Finally, an evaluation of the information-theoretic bound (1) is given in row (t).

4 Numerical Experiments

To illustrate the strength of the proposed design, we analyze the performance of some of the group-testing designs given in Table 2, when used to decode scintillation events in a PET setting.

4.1 Simulation parameters

In PET, scintillation crystals are used to convert 511 kilo-electron volt annihilation photons into bursts of low-energy (visible light) photons. We use the standard software package Geant4 [1, 46] to simulate this process for some 1,000 scintillation events for a $3 \times 3 \times 10$ mm^3 cerium-doped lutetium oxyorthosilicate (LSO) crystal (7.4 g/cm^3, $n = 1.82$, absorption length = 50 m, scintillation yield = 26,000 photons/MeV, fast time constant = 40 ns, yield ratio = 1, resolution scale = 4.41) coupled to a $3 \times 3 \times 0.75$ mm silicon sensor by 50μ of optical grease ($n = 1.5$, absorption length = 50m). For each event the simulation yields the location and arrival time of the low-energy photons with respect to the start of the event.

The silicon sensor is assumed to have a 70% fill factor and a quantum efficiency of 50% for blue photons. Once a photon is detected a pixel will be unable to detect a new photon for a known dead time, simulated to lie between 10 and 80 ns. We assume that each pixel takes up the same fraction of detector area and assign photons uniformly at random to a pixel. This increases the pixel firing rate by avoiding hitting dead pixels in high flux regions, thereby making the decoding process more challenging. We do not model dark counts and cross-talk between pixels, since they would account to less than 1% of the total number of detected photons and therefore do not significantly affect the result.

In terms of pixel firings, we ignore the jitter in the time between an incident photon and the actual firing of a pixel. This assumption greatly simplifies the simulation, and is not expected to have any significant influence on the results. The signal delays over the interconnection network between pixels and TDCs are assumed to be uniform, i.e., the travel time of the signal from each pixel to any connected TDC is assumed to be the identical, and can therefore be set to zero without loss of generality. TDCs are further assumed to be ideal in the sense that they have no down time; a time stamp is recorded whenever an event occurred during the sampling interval.

4.2 Decoding

Pixel firings give rise to specific patterns of TDC recordings through the group-testing design embedded in the interconnection network. These patterns can be decoded by considering the time stamps recorded in the memory buffer associated with each TDC and forming a binary test vector for each time interval. Given a test vector y, the decoding process starts by identifying all codewords a_i that are covered by y. When the group testing matrix A is a d-disjunct matrix, it immediately follows that whenever there are no more than d simultaneous firings, only the codewords corresponding to those pixels will be selected, and the decoding is successful. Whenever there are $s > d$ pixels that fired simultaneously, many more than s columns may be covered by y. If none of these columns can be omitted to form y then those columns coincide with pixels that fired and decoding is again successful. Otherwise, the decoding is ambiguous and considered unsuccessful. When decoding is successful we recover the pixels that fired, otherwise they are missed.

4.3 Results

In our simulations we considered sensors with both 60×60 and 120×120 pixel arrays, and a variety of different pixel dead times and TDC interval lengths. Due to space limitations we can only show a select number of tables that are representative of the results, and we will describe any significant differences in the text.

Table 4 shows the simulation results obtained using 60×60 and 120×120 arrays with interconnection networks based on the superimposed codes from Table 2, with disjunctness ranging from 2 to 6. The pixel dead time and TDC interval length are chosen to be 20 ns and 40 ps, respectively. These times are somewhat pessimistic; the typical dead time is longer, while the TDC interval could be shorter. Both choices cause an increase in the number of simultaneous photons per TDC sampling window, thereby making recovery more challenging. In particular, note that the maximum number of simultaneous firings reaches 14, far above the guaranteed recovery level. Nevertheless, it can be seen that even with a 4-disjunct interconnection network, more than 99% of all pixel firings are successfully recovered. For the 120×120 array, this number is slightly lower at 98.5% since fewer photons hit dead pixels, thus causing an increase in the number of firings and, consequently, an increase in the number of simultaneous hits.

A more complete picture on the relationship between the number of pixel firings missed and the pixel dead time and TDC interval length is given in Table 5. Shown are the percentage of pixel firings missed for various pixel dead times and TDC interval lengths. As expected, smaller TDC intervals reduce the number of simultaneous hits and therefore lead to more uniquely decodable events.

		Disjunctness (#TDCs)				
		$d = 2$ (51)	$d = 3$ (85)	$d = 4$ (142)	$d = 5$ (174)	$d = 6$ (206)
#Sim.	#Events	Decoded events (%)				
1	1,021,073	100.000	100.000	100.000	100.000	100.000
2	419,174	100.000	100.000	100.000	100.000	100.000
3	192,232	44.015	100.000	100.000	100.000	100.000
4	87,389	2.289	89.808	100.000	100.000	100.000
5	38,526	0.026	44.271	99.574	100.000	100.000
6	16,126	0.000	7.590	96.366	99.895	100.000
7	6,186	0.000	0.404	84.481	99.208	100.000
8	2,216	0.000	0.000	59.206	94.540	99.549
9	725	0.000	0.000	27.448	83.586	97.793
10	231	0.000	0.000	7.792	59.307	91.342
11	70	0.000	0.000	1.429	30.000	71.429
12	17	0.000	0.000	0.000	5.882	70.588
13	6	0.000	0.000	0.000	0.000	0.000
14	1	0.000	0.000	0.000	0.000	100.000
	#Pixel firings	Pixel firings missed (%)				
	3,145,990	32.571	9.636	0.833	0.135	0.025

(**a**) 60×60 pixel array

		Disjunctness (#TDCs)				
		$d = 2$ (63)	$d = 3$ (110)	$d = 4$ (161)	$d = 5$ (233)	$d = 6$ (323)
#Sim.	#Events	Decoded events (%)				
1	992,945	100.000	100.000	100.000	100.000	100.000
2	444,448	100.000	100.000	100.000	100.000	100.000
3	230,712	16.390	100.000	100.000	100.000	100.000
4	118,381	0.091	95.275	100.000	100.000	100.000
5	56,684	0.000	62.900	99.737	100.000	100.000
6	25,215	0.000	15.435	96.764	99.996	100.000
7	10,061	0.000	1.312	80.698	99.901	100.000
8	3,711	0.000	0.054	43.897	99.111	100.000
9	1,224	0.000	0.000	12.582	95.997	99.918
10	421	0.000	0.000	1.663	83.610	99.525
11	115	0.000	0.000	0.000	56.522	99.130
12	33	0.000	0.000	0.000	27.273	100.000
13	8	0.000	0.000	0.000	12.500	100.000
14	3	0.000	0.000	0.000	0.000	100.000
	#Pixel firings	Pixel firings missed (%)				
	3,599,359	44.554	10.326	1.430	0.068	0.001

(**b**) 120×120 pixel array

Table 4: Decoding statistics for two pixel arrays using a pixel dead time of 20ns and TDC interval length of 40ps. Results shown correspond to the decoding of 1,000 sequential scintillation events.

Dead time (#firings)	TDC interval	#Simult.	Pixel firings missed (%) $d=2$	$d=3$	$d=4$	$d=5$	$d=6$
10ns (3.4m)	5ps	6	1.32	0.02	0.00	0.00	0.00
	10ps	7	4.69	0.25	0.00	0.00	0.00
	20ps	11	14.48	1.87	0.04	0.00	0.00
	40ps	14	35.39	10.52	0.87	0.13	0.02
20ns (3.1m)	5ps	6	1.21	0.02	0.00	0.00	0.00
	10ps	7	4.31	0.23	0.00	0.00	0.00
	20ps	11	13.30	1.74	0.04	0.00	0.00
	40ps	14	32.57	9.63	0.83	0.13	0.02
40ns (2.8m)	5ps	6	1.22	0.03	0.00	0.00	0.00
	10ps	7	4.33	0.25	0.00	0.00	0.00
	20ps	11	13.21	1.83	0.05	0.00	0.00
	40ps	14	31.60	9.95	0.90	0.14	0.02
80ns (2.5m)	5ps	6	1.34	0.03	0.00	0.00	0.00
	10ps	7	4.73	0.28	0.00	0.00	0.00
	20ps	11	14.33	2.03	0.05	0.00	0.00
	40ps	14	33.83	11.04	1.00	0.16	0.03

(**a**) 60×60 pixel grid

Dead time (#firings)	TDC interval	#Simult.	Pixel firings missed (%) $d = 2$	$d = 3$	$d = 4$	$d = 5$	$d = 6$
10ns (3.7m)	5ps	6	2.27	0.02	0.00	0.00	0.00
	10ps	8	7.58	0.20	0.00	0.00	0.00
	20ps	12	21.33	1.69	0.08	0.00	0.00
	40ps	14	45.52	10.64	1.46	0.07	0.00
20ns (3.6m)	5ps	6	2.21	0.02	0.00	0.00	0.00
	10ps	8	7.39	0.20	0.00	0.00	0.00
	20ps	12	20.80	1.64	0.08	0.00	0.00
	40ps	14	44.55	10.33	1.43	0.07	0.00
40ns (3.5m)	5ps	6	2.20	0.02	0.00	0.00	0.00
	10ps	8	7.35	0.20	0.00	0.00	0.00
	20ps	12	20.62	1.66	0.08	0.00	0.00
	40ps	14	43.95	10.37	1.46	0.07	0.00
80ns (3.4m)	5ps	6	2.25	0.02	0.00	0.00	0.00
	10ps	8	7.50	0.20	0.00	0.00	0.00
	20ps	12	20.97	1.71	0.08	0.00	0.00
	40ps	14	44.46	10.64	1.50	0.07	0.00

(**b**) 120×120 pixel grid

Table 5: Percentage of pixel firings missed for various combinations of pixel dead time, TDC interval length, and disjunctness. Results shown correspond to the decoding of 1,000 sequential scintillation events. The first three columns show the dead time (and total number of pixel firings), TDC time interval, and maximum number of simultaneous hits, respectively.

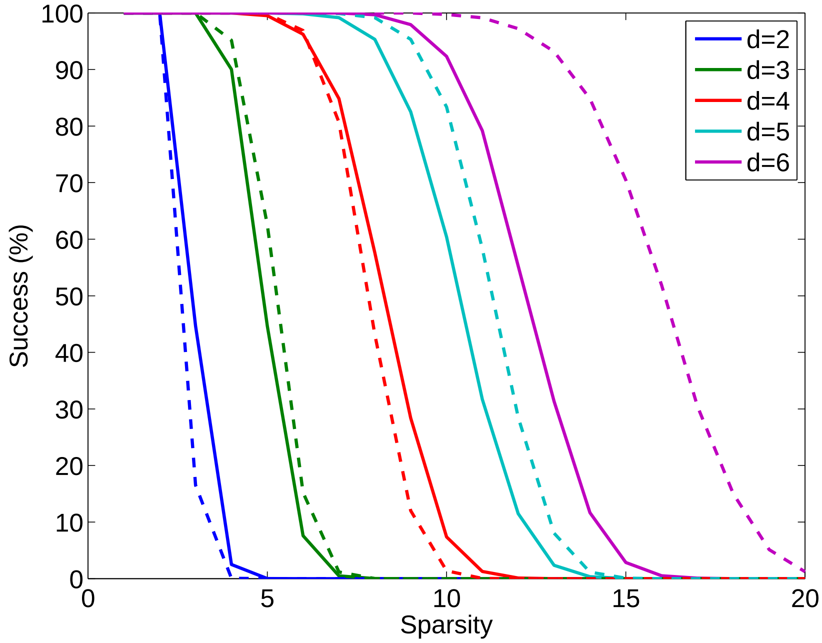

Figure 3: Percentage of successfully decoded vectors as a function of sparsity level for arrays of size 60×60 (solid) and 120×120 (dashed). For each sparsity level 10,000 random vectors were generated and decoded.

As seen, even when the number of simultaneous pixel firings exceeds the disjunctness of the group-testing design, it often remains possible to uniquely decode the resulting codeword. To get more accurate statistics, we studied the decoding properties of randomly generated sparse vectors (corresponding to random pixel firing patterns) with the number of nonzero entries ranging from 1 to 20. For each sparsity level we decoded 10,000 vectors and summarize the success rates in Figure 3. The plots show that recovery breaks down only gradually once the sparsity exceeds the disjunctness level of the matrix.

5 Discussion

For the adaptation of the group-testing based design in practical designs, a number of additional issues needs to be addressed. We discuss some of the major ones below.

Decoding. Since the TDCs store time stamps in a memory buffer, we can perform the decoding process off-line. This is analogous to the operation of a digital storage oscilloscope. Aside from the obvious benefit of reducing the amount of circuitry, it has the advantage that we have a global view of the entire data, not just the current event, or a short history of previous events. This data can be used to extract more information from unsuccessfully decoded events by excluding columns corresponding to pixels that fired shortly before or after the current event, or by using more sophisticated, but perhaps combinatorial decoding techniques.

Asynchronicity of the system. One challenge in the implementation of the proposed design is to make sure that the TDCs connected to a single pixel all record the firing of that pixel in the same

TDC interval. In other words, it is important that codewords are recorded in a single interval and not spread out over two consecutive intervals. Such a shift can occur due to differences of travel times of signals between the pixel and the TDCs as a result of differences in wiring lengths. The appearance of partial codewords in test vectors complicates decoding and may cause pixel firings to be masked by others and be missed completely with no means of detection.

There are two main approaches of dealing with this problem. The first approach is to synchronize the logical signal generated by the pixel using a global clock across the chip to ensure uniform arrival of signals to the TDC digitizers. Such an approach has been successfully implemented in clock design trees of CPU chips that maintain clock skews less than the TDC sampling frequency [44]. The second approach is to consider bursts of consecutive events and decode the union of the corresponding test vectors as a whole. This also leads to an increase in the expected number of simultaneous firings as well as a slight decrease in temporal resolution. This approach is possible only when the photon flux is sufficiently low; when many consecutive TDC windows contain events, their union simply contains too many pixel firings to be successfully decoded.

Acknowledgments

E. C., E. vdB., and C. S-L. would like to acknowledge support from the NSF via the Waterman Award; from the Broadcom Foundation; from the ONR via grant N00014-10-1-0599; and from AFOSR-MURI under grant FA9550-09-1-06-43. P.O. would like to acknowledge support through a Stanford Interdisciplinary Graduate Student Fellowship.

References

[1] S. Agostinelli et al. Geant4 – a simulation toolkit. *Nuclear Instruments and Methods in Physics Research Section A*, 506(3):250–303, 2003.

[2] N. Alon and J. H. Spencer. *The Probabilistic Method*. Wiley Series in Discrete Mathematics and Optimization. Wiley, New York, 1992. (2nd Edition, 2000).

[3] B. F. Aull, A. H. Loomis, D. J. Young, R. M. Heinrichs, B. J. Felton, P. J. Daniels, and D. J. Landers. Geiger-mode avalanche photodiodes for three-dimensional imaging. *Lincoln Laboratory Journal*, 13(2):335–350, 2002.

[4] D. J. Balding, W. J. Bruno, E. Knill, and D. C. Torney. A comparative survey of non-adaptive pooling designs. In T. P. Speed and M. S. Waterman, editors, *Genetic Mapping and DNA Sequencing*, pages 133–154. Springer, 1996.

[5] Z. Baranyai. On the factorization of exponential sized families of k-independent sets. In *Proc. Colloq. Math. Soc. János Bólyai, 10th, Infinite and Finite Sets*, 1973.

[6] A. E. Brouwer. Bounds for constant weight codes. Available online at `http://www.win.tue.nl/~aeb/codes/Andw.html`.

[7] I. F. Castro, A. J. Soares, and J. F. Veloso. Impact of dark counts in low-light level silicon photomultiplier multi-readout applications. In *2009 IEEE Nuclear Science Symposium Conference Record (NSS/MIC)*, pages 1592–1596, November 2009.

[8] S. Chaudhuri and J. Radhakrishnan. Deterministic restrictions in circuit complexity. In *Proceedings of the twenty-eighth annual ACM symposium on Theory of computing*, STOC '96, pages 30–36, New York, NY, USA, 1996. ACM.

[9] Y. Cheng and D.-Z. Du. New constructions of one- and two-stage pooling designs. *Journal of Computational Biology*, 15:195–205, 2008.

[10] A. E. Clementi, A. Monti, and R. Silvestri. Distributed broadcast in radio networks of unknown topology. *Theoretical Computer Science*, 302(1–3):337–364, 2003.

[11] R. Clifford, K. Efremenko, E. Porat, and A. Rothschild. k-mismatch with don't cares. In *Proceedings of the 15th annual European conference on Algorithms*, ESA'07, pages 151–162, Berlin, Heidelberg, 2007. Springer-Verlag.

[12] C. J. Colbourn and J. H. Dinitz. *Handbook of Combinatorial Designs*. Discrete Mathematics and Its Applications. Chapman & Hall/CRC, 2007. Series Editor: Kenneth H. Rosen.

[13] G. Cormode and S. Muthukrishnan. Combinatorial algorithms for compressed sensing. In P. Flocchini and L. Gasieniec, editors, *Structural Information and Communication Complexity*, volume 4056 of *Lecture Notes in Computer Science*, pages 280–294. Springer Berlin / Heidelberg, 2006.

[14] A. De Bonis, L. Gąsieniec, and U. Vaccaro. Optimal two-stage algorithms for group testing problems. *SIAM Journal on Computing*, 34(5):1253–1270, 2005.

[15] A. De Bonis and U. Vaccaro. Constructions of generalized superimposed codes with applications to group testing and conflict resolution in multiple access channels. *Theoretical Computer Science*, 306(1–3):223–243, 2003.

[16] R. Dorfman. The detection of defective members of large populations. *The Annals of Mathematical Statistics*, 14(4):436–440, 1943.

[17] D.-Z. Du and F. K. Hwang. *Combinatorial Group Testing and Its Applications*. World Scientific Publishing Company, 2000.

[18] D. Z. Du and F. K. Hwang. *Pooling Designs and Nonadaptive Group Testing: Important Tools for DNA Sequencing*, volume 18 of *Series on Applied Mathematics*. World Scientific, New York, 2006.

[19] A. G. D'yachkov, A. J. Macula, and V. V. Rykov. New constructions of superimposed codes. *IEEE Transactions on Information Theory*, 46:284–290, 2000.

[20] A. G. D'yachkov, A. J. Macular, and V. V. Rykov. *New Applications and Results of Superimposed Code Theory Arising from the Potentialities of Molecular Biology*, chapter 22, pages 265–282. Kluwer Academic Publishers, 2000.

[21] A. G. D'yachkov and V. V. Rykov. A survey of superimposed code theory. *Problems of Control and Information Theory*, 14:1–13, 1983.

[22] D. Eppstein, M. T. Goodrich, and D. S. Hirschberg. Improved combinatorial group testing algorithms for real-world problem sizes. *SIAM Journal on Computing*, 36(5):1360–1375, 2007.

[23] P. Erdös, P. Frankl, and Z. Füredi. Families of finite sets in which no set is covered by the union of two others. *Journal of Combinatorial Theory, Series A*, 33(2):158–166, 1982.

[24] P. Erdös, P. Frankl, and Z. Füredi. Families of finite sets in which no set is covered by the union of r others. *Israel J. Math.*, 51:79–89, 1985.

[25] P. Erdös and L. Lovász. Infinite and finite sets. *Colloq. Math. Soc. Jãnos Bolyai*, 10:609–627, 1974.

[26] M. Farach, S. Kannan, E. Knill, and S. Muthukrishnan. Group testing problems with sequences in experimental molecular biology. In *Proceedings of Compression and Complexity of Sequences 1997*, pages 357–367, June 1997.

[27] T. Frach, G. Prescher, C. Degenhardt, R. de Gruyter, A. Schmitz, and R. Ballizany. The digital silicon photomultiplier – principle of operation and intrinsic detector performance. In *2009 IEEE Nuclear Science Symposium Conference Record (NSS/MIC)*, pages 1959–1965, October 2009.

[28] Z. Füredi. On r-cover-free families. *Journal of Combinatorial Theory, Series A*, 73:172–173, 1996.

[29] D. Gordon et al. La Jolla Covering Repository. Available online at `http://www.ccrwest.org/cover.html`.

[30] M. Grassl. Bounds on the minimum distance of linear codes and quantum codes. Available online at `http://www.codetables.de`, 2007.

[31] D. Henseler, R. Grazioso, N. Zhang, and M. Schmand. SiPM performance in PET applications: An experimental and theoretical analysis. In *Nuclear Science Symposium Conference Record (NSS/MIC), 2009 IEEE*, pages 1941–1948, November 2009.

[32] F. K. Hwang and V. T. Sós. Non adaptive hypergeometric group testing. *Studia Sci. Math. Hungarica*, 22:257–263, 1987.

[33] P. Indyk. Deterministic superimposed coding with applications to pattern matching. In *Proceedings of the 38th Annual Symposium on Foundations of Computer Science*, pages 127–136, Washington, DC, USA, 1997. IEEE Computer Society.

[34] S. Isaak, M. C. Pitter, S. Bull, and I. Harrison. Design and characterisation of 16×1 parallel outputs SPAD array in 0.18 um CMOS technology. In *2010 IEEE Asia Pacific Conference on Circuits and Systems (APCCAS)*, pages 979–982, December 2010.

[35] S. M. Johnson. Improved asymptotic bounds for error-correcting codes. *IEEE Transactions on Information Theory*, 9(4):198–205, 1963.

[36] W. H. Kautz and R. C. Singleton. Nonrandom binary superimposed codes. *IEEE Transactions on Information Theory*, 10(4):363–377, October 1964.

[37] E. Knill, W. J. Bruno, and D. C. Torney. Non-adaptive group testing in the presence of errors. *Discrete Applied Mathematics*, 88(1–3):261–290, November 1998.

[38] A. J. Macula. Error-correcting nonadaptive group testing with d^e-disjunct matrices. *Discrete Applied Mathematics*, 80(2–3):217–222, December 1997.

[39] F. J. MacWilliams and N. J. A. Sloane. *The Theory of Error-Correcting Codes*. North-Holland Publishing Company, Amsterdam, 1977. (3rd printing, 1983).

[40] B. Markovic, A. Tosi, F. Zappa, and S. Tisa. Smart-pixel with SPAD detector and time-to-digital converter for time-correlated single photon counting. In *2010 23rd Annual Meeting of the IEEE Photonics Society*, pages 181–182, November 2010.

[41] H. Q. Ngo and D.-Z. Du. A survey on combinatorial group testing algorithms with applications to DNA library screening. In *Discrete Mathematical Problems with Medical Applications*, volume 55 of *DIMACS Ser. Discrete Math. Theoret. Comput. Sci.*, pages 171–182, Providence, RI, 2000. American Mathematical Society.

[42] E. Porat and A. Rothschild. Explicit non-adaptive combinatorial group testing schemes. In L. Aceto, I. Damgård, L. Goldberg, M. Halldórsson, A. Ingólfsdóttir, and I. Walukiewicz, editors, *Automata, Languages and Programming*, volume 5125 of *Lecture Notes in Computer Science*, pages 748–759. Springer Berlin / Heidelberg, 2008.

[43] D. Renker. Geiger-mode avalanche photodiodes, history, properties and problems. *Nuclear Instruments and Methods in Physics Research Section A: Accelerators, Spectrometers, Detectors and Associated Equipment*, 567(1):48–56, 2006.

[44] P. J. Restle, T. G. McNamara, D. A. Webber, P. J. Camporese, K. F. Eng, K. A. Jenkins, S. Member, D. H. Allen, M. J. Rohn, M. P. Quaranta, D. W. Boerstler, C. J. Alpert, C. A. Carter, R. N. Bailey, J. G. Petrovick, B. L. Krauter, and B. D. McCredie. A clock distribution network for microprocessors. *IEEE Journal of Solid-State Circuits*, 36(5):792–799, May 2001.

[45] L. Riccio and C. J. Colbourn. An upper bound for disjunct matrices. Preprint, University of Vermont, 1998.

[46] P. Rodrigues, R. Moura, C. Ortigão, L. Peralta, M. G. Pia, A. Trindade, and J. Varela. Geant4 applications and developments for medical physics experiments. *IEEE Transactions on Nuclear Science*, 51(4):1412–1419, August 2004.

[47] M. Ruszinkó. On the upper bound of the size of the r-cover-free families. *Journal of Combinatorial Theory, Series A*, 66:302–310, 1994.

[48] F. Sefkow. The CALICE tile hadron calorimeter prototype with SiPM read-out: Design, construction and first test beam results. In *Nuclear Science Symposium Conference Record, 2007. NSS '07. IEEE*, volume 1, pages 259–263, November 2007.

[49] R. C. Singleton. Maximum distance q-nary codes. *IEEE Transactions on Information Theory*, 10(2):116–118, April 1964.

[50] M. Sobel and P. A. Groll. Group testing to eliminate efficiently all defectives in a binomial sample. *Bell Syst. Tech. J.*, 38:1179–1252, 1959.

[51] W. A. Stein et al. *Sage Mathematics Software (Version 4.7.2)*. The Sage Development Team, 2012. `http://www.sagemath.org`.

[52] M. Teshima, B. Dolgoshein, R. Mirzoyan, J. Nincovic, and E. Popova. SiPM development for astroparticle physics applications. In *Proceedings of the 30th International Cosmic Ray Conference*, volume 5, pages 985–988, 2007.

[53] J. K. Wolf. Born again group testing: Multiaccess communications. *IEEE Transactions on Information Theory*, 31(2):185–191, March 1985.

[54] H.-G. Yeh. d-Disjunct matrices: Bounds and Lovász local lemma. *Discrete Mathematics*, 253(1–3):97–107, June 2002.